Accurate and early detection of poplar tree leaf spot disease using image processing technique

Shahryar Sedighi[1], Davood Kalantari[1*], Saeid Shiukhy[2], Jozef Rédl[3]

(1. Department of Biosystems Engineering, Faculty of Agricultural Engineering, Sari Agricultural Sciences and Natural Resources University (SANRU), Iran;

2. Department of Water Engineering, Faculty of Agricultural Engineering, Sari Agricultural Sciences and NaturalResources University (SANRU), Iran;

3. Department of Machine Design, Faculty of Engineering, SAU in Nitra, Slovak Republic)

Abstract: Leaf spot disease is one of the most common fungal diseases that cause immense and sometimes irreparable damage to poplar trees. In this regard, conventional methods for detection of fungal contamination are time-consuming, costly and difficult. Therefore, in this study, in order to distinguish healthy leaves from infected ones, a modified image processing algorithm by using the Laplacian threshold was used. In this study, the illumination wavelengths have been selected using a UV-Visible Spectrophotometer device (PG Instruments, Model T92+ Double® Beam, England). The images were recorded using a 1260 lux light intensity and a digital camera mounted on the stereomicroscope (SN 287050, Italy) with a resolution of 5 megapixels. The experimental data were analyzed based on a completely randomized design with three replications. Analysis of variance (ANOVA) test was used to determine the significance of treatments performance. According to the results, the red spectrum with 680nm wavelength showed the highest contaminated surface on the leaf (190500 μm^2). In contrast, the yellow spectrum with a wavelength of 585 nm determined the lowest amount of contaminated surface (65781 μm^2). The blue and green spectra showed roughly the same performance in early detection of fungal contamination. Overall obtained results showed that the red spectrum with wavelength of 680 nm is more reliable for early poplar leaves' surface contamination detection in compare to blue (470 nm), green (550 nm) and yellow (585 nm) wavelengths with 13%, 14% and 55.8% improvements, respectively. The method presented in this study can be used to identify the quality and the health of biological products and disease progression, significantly easier and faster in compare to the conventional methods.

Keywords: image processing, machine vision, poplar tree, wavelength

Citation: Sedighi, S., D. Kalantari, S. Shiukhy, and J. Rédl. 2021. Accurate and early detection of poplar tree leaf spot disease using image processing technique. Agricultural Engineering International: CIGR Journal, 23(2):170-180.

1 Introduction

The poplar species (Populous L) belong to the willow family (salicaceae). Unfortunately, poplar species are prone to a variety of diseases. Diseases of this plant range from roots to leaves, with the leaf spot disease being its most important diseases (Babai-Ahri et al., 2016; Erickson et al., 2003). The leaf spot disease reduces photosynthesis in the leaf and ultimately reduces growth and even causes plant death (Maxwell et al., 1997). Symptoms of the disease appear as necrotic scars on the leaf lamina, which causes aging and premature loss of leaves (Erickson et al.,

Received date: 2020-05-03 **Accepted date:** 2020-11-01
***Corresponding author: Davood Kalantari,** (lecture, professor, etc), Department of Biosystem Engineering, Faculty of Agricultural Engineering, Sari Agricultural Sciences and Natural Resources University (SANRU), Iran. Email: d.kalantari@sanru.ac.ir.

2003).

The serious research on poplar has been started in Iran since 1955 with Iran joining the International Poplar Commission (IPC) and started subsequent studies on genetic modification, transplantation, pest and disease identification, and exploitation.

Symptom detection by experts is time consuming and often too late for curative treatments. With imaging technologies site-specific application systems as for example against grape downy mildew could be established (Oberti et al., 2016).

In parallel to the expanding various methods of image analysis in industry, the application of this method in modern agriculture is also expanding, see e.g., Habib et al. (2020), Rezaei et al. (2019). This technique is one of the most important methods for evaluation of agricultural products, classification of weed, and its applications are expanding with development and advancement of hardware and software of image processing systems (Hemming and Rath, 2001). Nowadays, image analyzing based on machine vision is widely used in evaluation of crops and orchards, crop grading systems, color detection, appearance defects, and defects in the tissue of the crops and diseases were identified before visible symptoms developed (Lowe et al., 2017). The most important advantages of this method are the speed of the product's descriptive data generation, user's workload reduction, being economical and easy to use, non-destructive and harmless, and having a stable control system and precise performance, meanwhile has its drawbacks, see e.g., Moya et al. (2005). For example, the lighting system in this method must be very accurate, which means in different environments, the results could be different. Furthermore, it is very difficult to work with images in dim and dark conditions. As mentioned above, it is very important to optimize the lighting indexes to get the proper output from the performance of devices equipped with this set of capabilities, and in addition to the degrees of freedom of the device, it is very important to determine the specific optical spectra for high efficiency.

In the machine vision applications, two subjects should be considered, which knowing and understanding both of these factors can influence the results of machine vision in agricultural automation; first being the visual and physical indices of the plant such as color, dimensions, and geometry of the crop and even its temperature and the second being the elements associated with the light source and the way it reflects from the surface of the plant, see e.g., orange detection on tree using digital image processing based on neural network method and light shading density (Ahmadi and Amiri Pariyan, 2014).

To study the propagation process of pear crush volume due to static loading, Razavi et al. (2020) used image processing techniques with Image J software to measure the pear crush volume. Based on their results, increased strain energy resulted mechanical hysteresis and hysteresis loss and pear crush volume. Additionally, increasing the elasticity of the treatments yield reduction in crush volume of the loaded samples. As the storage period increased, propagation of the crush volume was slightly altered, which was well recorded by calculating the crushing volume propagation process using image processing technique.

By using image processing, Bakhshipour-Ziyaratgahi et al. (2016) showed that in a system, the machine vision is capable of distinguishing the crops from the weeds. To this end, the distinguishing features between the main plant and the weed must first be identified. In this study, by analyzing various pictures of beetroots, a particular shape on the beetroot's leaves and a particular feature of it which was distinguishable from the common weeds were determined. This feature was a curved petiole, which was exclusive to the beetroot that presented as the S algorithm to the system. Investigating the results of this method which was conducted on 7/8 pictures from the beetroots, showed 92% of conformity.

Zhang et al. (2017) presented a method that in addition to curing, can identify cucumber leaves' pests by image processing technique. In this study, the SR principle was used to diagnose the disease by first converting the image

of the cucumber's leaf into a l*a*b model and drawing its histograms using the Fourier Transform (FT) Function. In the next step of analyzing the results, the Gray-level mode was extracted. Applying constraints on the decomposition of infected areas, an algorithm was proposed to detect the type of disease after passing through the previous steps according to the graphs. The SR method was up to 85.7% more accurate in detecting the disease in compare to the conventional methods.

The experimental investigation provided by Fahrentrapp et al. (2019) showed that Near Infra-Red (NIR) and Red Edge (RE) are as the two most informative spectral data sets to differentiate pathogen- and mock-inoculated leaf regions of interest (ROI). They recorded in time-course experiments of detached tomato leaves inoculated with the fungus Botrytis cinerea and mock infection solution, using a five-lens multispectral imager, spectral reflectance of green, blue, red, near infrared (NIR, 840 nm), and red edge (RE, 720 nm). Their concluding result indicated that gray mold leaf infections could be identified at the earliest at 9h post infection (hpi) in the most informative bands NIR and RE.

Foliar surface diseases such as leaf spots, are one of the most common fungal diseases that decrease photosynthesis, leaves efficiency and consequently decreases the growth rate of the poplar tree. Therefore, in order to prevent the development of this fungal disease and reduce its losses, it is essential to identify and eliminate its pathogens. In this regard, using conventional methods for the detection of fungal contamination is very time consuming, expensive and difficult. Therefore, in this study, a fast and reliable method based on machine vision technology is used to identify infected leaves and also to determine the rate of the infection progress. Furthermore, the effect of four different wavelengths of illumination for the accurate and early detection of poplar leaf spot disease was investigated and examined.

2 Materials and methods

In this study, poplar leaf's images from the white poplar species (P. Alba L.) with the symptoms of the early disease were collected from Sari Agriculture Sciences and Natural Resources University (Latitude: 36°66′09″ N, Longitude: 53°07′13″ E, and elevation above sea level: 8 m) on the 23rd of July, 2019. According to the previous researches, see e.g., Babai-Ahri et al. (2016), this type of disease may affect the leaf from the beginning of the leaf growth, and remain on it until the deciduous season, causing the plant to slow its growth by reducing adequate light absorption.

In the current research, the leaves were collected at the beginning of their maturity, i.e. after their initial growth and reaching their maximum size. In this time, it was possible to early visualize the initial leaf spot disease using the stereomicroscopic images. The images were recorded under the same conditions of lighting emitted from the light source. Images were recorded in a black chamber (50×50 cm) to maximize light source reflections and to avoid noise with 1260 lux light intensity and with a digital camera mounted on the stereomicroscope (SN 287050 Model, Italy) with a resolution of 5 megapixels at 2592×1944 resolution. In all images, a scale index was used in the Image J software at room temperature measured by a 994 μm-sized micrometer. The camera was connected to the computer with a USB cable and images were stored in the RGB mode using Future Winjoe software. In this experiment, images in four spectra (with different wavelengths) were used to identify the appropriate wavelength for image processing, including blue (470 nm), green (550 nm) and yellow (585 nm) and red (680 nm).

The spectra were examined in a UV-Visible Spectrophotometer device (PG Instruments, Model T92+ Double® Beam, England) to measure the wavelengths of visible spectra used in the experiments (Figure 1-a). This device compares the intensity of light passing through the sample (I) and the intensity of the initial scattered light from the sample (I_0). The (I/I_0) ratio is generally expressed as T% and thus the absorption rate is obtained on this basis (Equation 1).

$$A = -log(\%T/100\%) \quad (1)$$

(a) (b)

Figure 1 The laboratory equipment, a) Spectrometer to determine wavelength of absorption spectrum, b) using stereomicroscope and camera mounted on it to obtain leaf surface images

Using spectrophotometer, spectral absorption curves were obtained to determine the wavelength (Figure 2). In this graph, the wavelength varied based on the absorption values for each spectrum. For each spectrum, the transmitted wavelength was obtained as the wavelength associated with the lowest absorption rate. For the blue spectrum, the highest absorbance was at 333 nm, with the smallest absorbance after that being 470 nm. Accordingly, the wavelengths of all the spectra tested in the illumination process were obtained according to Figure 2, with red, green and yellow had wavelengths of 680, 550 and 585 nm, respectively.

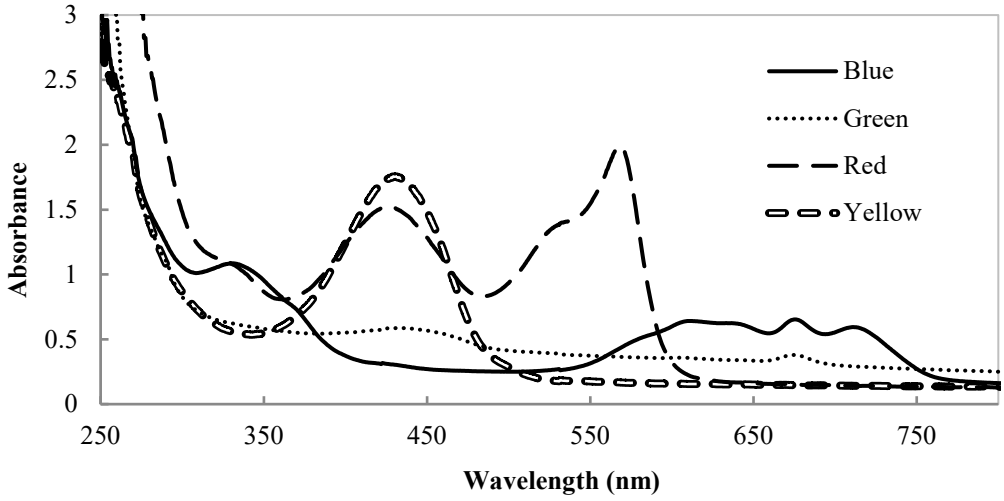

Figure 2 Spectral absorption curve for determination of wavelength

The images were then transferred from the stereomicroscope to the Image J software environment. The selected treatment was based on preliminary observations of fungal disease and randomly, parts of it were examined (Figure 3). The methodology used in this study was similar to the method utilized by Fahrentrapp et al. (2019) and Lowe et al. (2017).

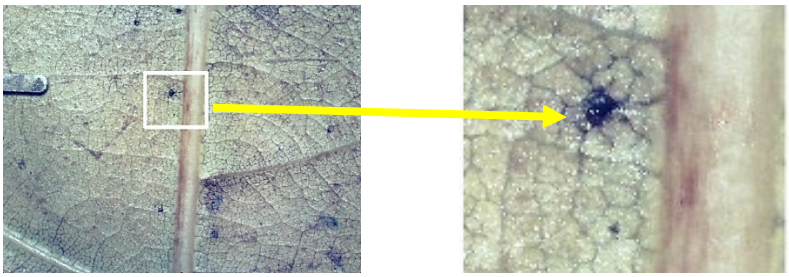

(a) (b)

(a) normal image with no magnification,(b) zoomed area

Figure 3 Surface image on leaf

In the images transferred to the Image J software, the index size was first determined by specifying a scale on the images in the software from the Analyze section and then activating this scale in nanometer-pixels for all the images.

Then, by determining an 8-bit resolution, the RGB images were converted to grayscale images to eliminate the noise due to the illumination or ambient light in the images and to continue the image processing process more accurately (Payman et al, 2016). The grayscale image can be represented by the two-dimensional function $f(x, y)$, where x and y are the spatial coordinates and the value of f is the brightness of the image at that point. When the values of x and y and the values of $f(x, y)$ are expressed in finite and discrete values, the image is then called a digital image. Digitizing the values of x and y is called Sampling and digitizing the value of $f(x, y)$ is called quantization.

The edge detection and its detection threshold were determined according to the Laplacian Operator (Equation 2) and by changing the brightness of the pixels in both horizontal and vertical directions, the desired boundary in the images was determined (Yan et al., 2020).

$$\left|\overrightarrow{\nabla f}\right| = |f_x| + \left|f_y\right| = [(\partial f/\partial x)^2 + (\partial f/\partial y)^2]^{1/2} \quad (2)$$

In this equation, x and y are the location coordinates of each pixel and f is the brightness of the image in that pixel. In Equation 2, $\partial f/\partial x$ is the brightness gradient in the x direction and $\partial f/\partial y$ is the brightness gradient in the y-direction. By this definition, if the mean sum of the squares of the brightness exceeds a default value in two directions, it can be recognized as a criterion for detecting the boundary of objects or objects within the image (Dabbaghi et al., 2018). This criterion is known as the boundary threshold detection. Comparison of common edge detector algorithms to detect edges in non-cracked and rough cracked seeds is given in Dabbaghi et al. (2018). As a result, if the edges of an image are detected, the location of all objects in that image will be specified. A two-dimensional matrix with M rows and N columns (M×N) was used to display the image (Polder et al., 2003). The value of each array indicated the brightness of the image at that point. Each array is an 8-bit value that can have values between zero and 255. A value of 255 indicates absolute dark (black) and a value of zero indicates absolute light (white). The resulting image size was 2592×1944, which means a 2592-row and 1944-column matrix was used to display the image. Each pixel in this image also had a value between zero and 255. Bright spots have values close to zero and dark points have values close to 255. These values were used in image processing functions and the necessary mathematical operations were performed on the image.

Next, the contrast of the received image was changed to increase the difference between the minimum and maximum brightness levels. The term gray surface also refers to the brightness of monochrome images. According to the results of previous researches, see e.g., Payman et al. (2016), the gray intensity of the image depends on the number of minerals in the leaf surface which affects the wavelength of the spectrum emanating from each image. By decreasing the contrast, the pathogen or its progress was examined, which was focused on the visible wavelength range. Since only a part of the leaf involved with the disease was considered in the present study, in the software's threshold section, the threshold value for all optical spectra was (similarly) adjusted so that the infected or suspected for infection of the leaf was removed from its healthy parts. Finally, by applying a specified threshold, the images were converted to binary (black and white) mode (Izadi et al., 2016) (Figure 4).

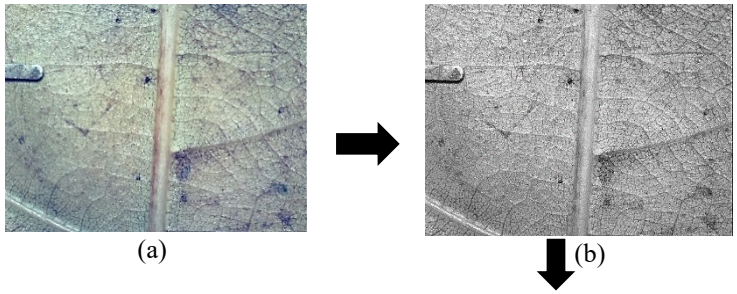

(a) (b)

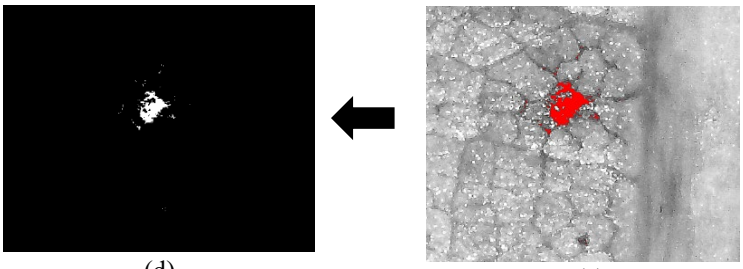

(d) (c)

a) raw image, b) gray image, c) crop threat area, d) binary image

Figure 4 The process of forming a binary image with a defined threshold

A four-step algorithm with limitations was used to determine the largest infection levels or suspected levels for infection to reduce the amount of error in detecting the area involved while identifying the main pathogen of this disease to convert and count of contaminated spots by applying certain constraints . The steps of implementing the algorithm are as follows: 1) preprocessing in a specified scale, 2) determining the same threshold for all treatments, 3) imposing limits on the detection of points, and 4) displaying the largest disease areas and counting them. A similar image-processing based algorithm to automatically identify plant disease was developed by Camargo and Smith (2009).

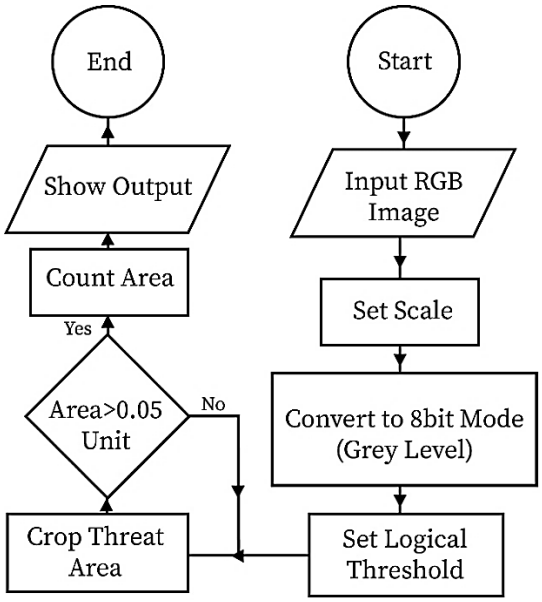

Figure 5 The algorithm flowchart for image conversion and counting of contaminated spots by applying certain constraints

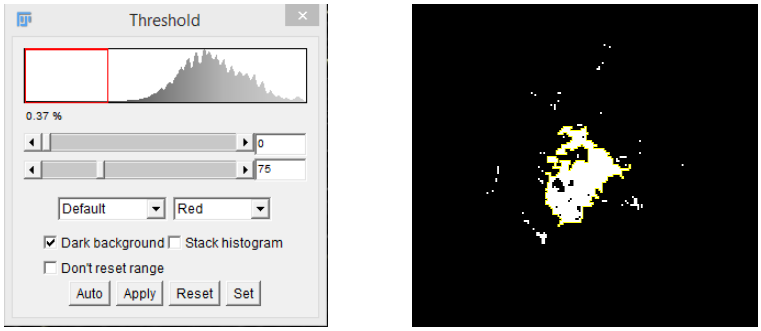

(a) (b)

Figure 6 applying threshold on histogram chart, a) Designated area, b) largest detection area

The algorithm was first applied to the largest contamination area of the treatments. According to the changes in image contrast, a 0.37% threshold (Figure 6-a) was chosen, so that by finalizing the threshold value, healthy areas became absolute black (255) and infected areas or suspected areas of infection became absolute white (0) (Figure 6-b). In addition to calculating the largest area involved in each treatment, this algorithm was also used to count the infected points for each treatment.

Figure 7 is an example of a raw image obtained from a camera mounted on a stereomicroscope showing an 8-bit image, an image due to applying the threshold, and the final binary image for detecting surface disease at different wavelengths.

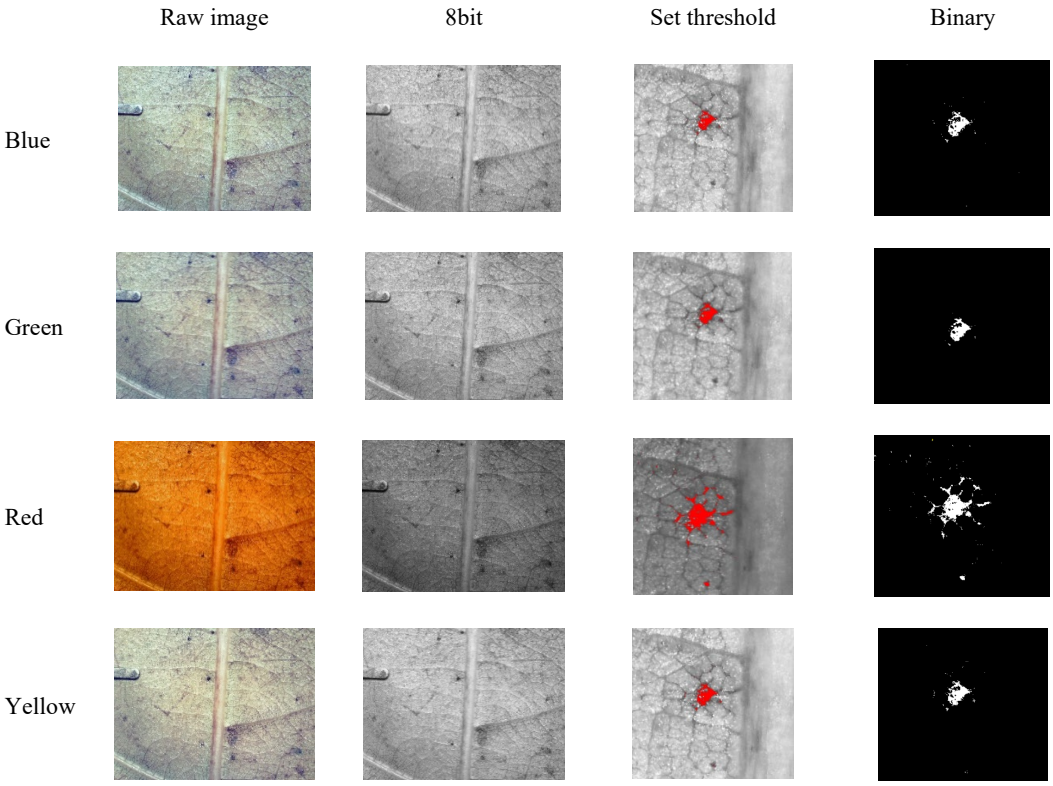

Figure 7 Exemplary of raw image obtained from a camera mounted on a stereomicroscope, 8-bit image, image after applying the threshold, and the final binary image for detecting surface disease at different wavelengths

The experiments were performed based on a completely randomized design with three replications using the SAS 9 software. The treatments were four different color spectrums of illumination whose effects were studied on the level of contamination detection on the leaves.

3 Results and discussion

The results of the analysis of variance of the parameter measured by the factors under test are presented in Table 1. In this analysis of variance (ANOVA) test was used to determine the significance of treatments performance. According to the proposed algorithm, the results showed that for each spectrum, the number of counted elements had a meaningful difference and this algorithm was successful in detecting and displaying the largest contamination points.

Table 1 Investigation of statistical results for the largest contaminant areas (areas greater than 1000 μm^2)

Source of variation	SS	Df	MS (area(μm^2))	F	Sig
Between spectrums	20783824600.59	3	6927941533.53*	10444.98	.00
Within spectrums	7959350.75	12	663279.23*		
Total	20791783951.35	15			

Note: * Significant at 5% probability level.

This test showed that the mean performance of each spectrum in detecting contaminated surfaces has a meaningful difference at a 5% probability level.

After determining the meaningful test presented in Table 1, the difference in detection of the area affected by leaf spot disease with an area greater than 1000 μm^2 is shown in Table 2. Each spectrum was compared using Least Significant Difference (LSD) test and its standard error was determined. According to the results of Table 2, the wavelength of the blue spectrum performed better than the green and yellow wavelengths in detecting the involved edge to the disease and thus the area involved in the disease (μm^2) had a better efficiency, but its performance was lower than the wavelength of the red spectrum with 680 nm wavelength. Based on the results shown in Table 2, the green spectrum has the lowest performance and the red spectrum has the best performance in detecting the edge of the surfaces involved with the contaminated surface, see e.g., Fahrentrapp et al. (2019).

Table 2 Investigate the significant differences between each treatment and compare each treatment with the other treatments

Spectrum		Mean difference	Std. Error	Sig.		
(i)	(j)				Lower bound	Upper bound
	green	61557.77*	575.88	.000	60303.03	62812.51
blue	red	-19797.46*	575.88	.000	-21052.2025	-18542.72
	yellow	60049.84*	575.88	.000	58795.1063	61304.58
	blue	-61557.77*	575.88	.000	-62812.5132	-60303.03
green	red	-81355.23*	575.88	.000	-82609.9775	-80100.50
	yellow	-1507.93*	575.88	.022	-2762.6687	-253.19
	blue	19797.46*	575.88	.000	18542.7260	21052.20
red	green	81355.23*	575.88	.000	80100.5010	82609.97
	yellow	79847.30*	575.88	.000	78592.5705	81102.04
	blue	-60049.84*	575.88	.000	-61304.5827	-58795.10
yellow	green	1507.93*	575.88	.022	253.1923	2762.66
	red	-79847.30*	575.88	.000	-81102.0470	-78592.57

Note: * Significant at 5% probability level.

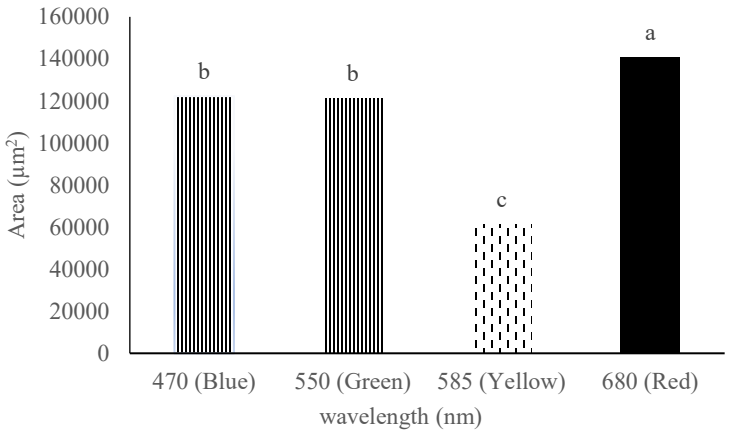

Figure 8 Performance of different spectra in identifying the greatest contamination area on the leaf

Figure 8 shows the performance of different spectra in identifying the greatest contamination area on the leaf. According to the results shown in this figure, there is no meaningful relation between the wavelength increase and the area detection of the largest area of contamination on the leaf, so that by increasing the wavelength of illumination from 470 to 550 nm, no meaningful difference between the wavelength increase and largest contamination area detection on the leaf was observed. Then, by increasing the wavelength from 550 to 585nm, determining the involved area with the disease was reduced, and eventually, by increasing the illumination wavelength from 585 to 680 nm, the process of detecting the involved area with the disease was increased.

To determine the disease progression at the leaf's surface, a test was performed to count the number of infected points on the leaf surface. This test determines the process of disease development at the leaf surface. According to the results shown in Figure 9, the red spectrum, with better edge detection, detected more points in compare to the other spectra. The dependence of the detected values on the wavelength of the spectrum was in a way that the lower wavelength spectra such as yellow, blue, and green spectra did not correctly distinguish the difference between the edge of the healthy and contaminated points, and according to Equation 2, the software counted fewer surfaces than the wavelength of the red spectrum (680 nm).

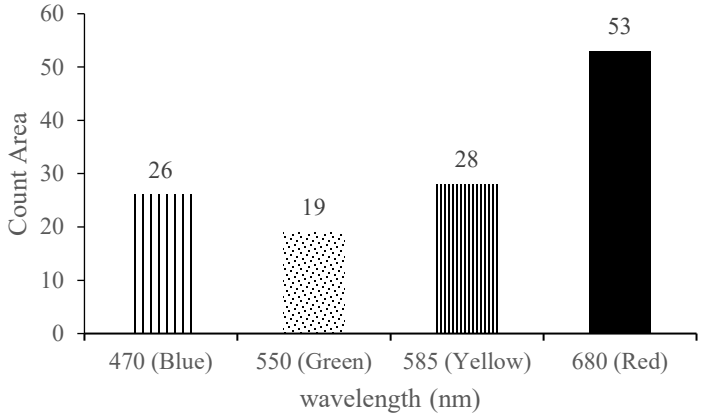

Figure 9 Total number of detected contaminated points on the leaf for each spectrum at the threshold (0.37%)

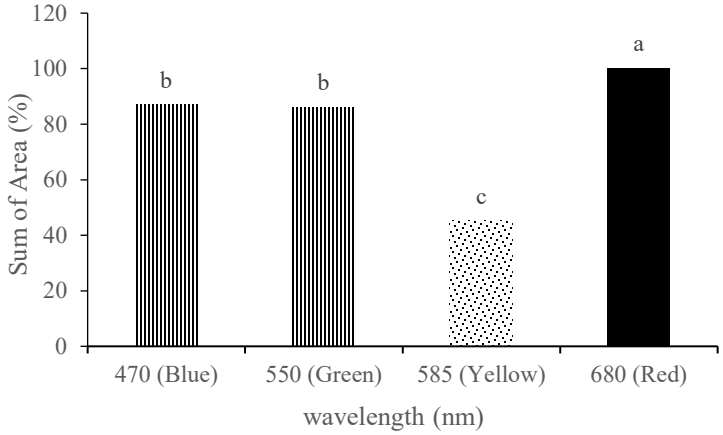

Figure 10 The sum of the detected areas for each spectrum

For the final evaluation, sum of the detected areas for each spectrum was calculated and presented in Figure 10. According to the results shown in this figure, the blue and green spectra showed the same performance with the sum of the close disease-related levels, and the difference in the areas of disease-related levels was not meaningful at 5%

probability level. Based on the results shown in Figure 10, the red spectrum with 680 nm wavelength showed the highest contaminated surface on the leaf (190500 μm^2). In contrast, the yellow spectrum with a wavelength of 585 nm determined the lowest amount of contaminated surface (65781 μm^2).

4 Conclusion

The overall results of the presented study showed that image processing technique has high potential in early determining and diagnosing disease factors in plants. This procedure is fast, less costly and also non-destructive than other methods such as plant tissue chemical analysis. Using the 680 nm wavelength in compare to 470, 550 and 585 nm, indicated 13%, 14%, and 55.8% improvement in detecting the primarily involved surface and the disease's progression rate, respectively, which is due to the more accurate edge detection according to the Laplacian Operator. According to the statistical results, the wavelengths of the red spectrum showed the best performance with the best representation of the largest area involved, progression process and the number of counts, while the green and yellow wavelengths showed poor performance in these cases. Therefore, it is suggested that higher wavelength spectra for illumination in image processing operations can be used in laboratories or machine vision to make the detection of leaf surface diseases more accurate and less error-prone.

Acknowledgment

This project has been supported by the European Union (EU) under Erasmus+ project entitled "Fostering Internationalization in Agricultural Engineering in Iran and Russia [FARmER] with grant number 585596-EPP-1-2017-1-DE-EPPKA2-CBHE-JP, which is acknowledged.

References

Ahmadi, H. R., and J. Amiri Pariyan. 2014. Confirm the title, Orange Recognition on Tree Using Image Processing Method Based on Lighting Density Pattern. *Journal of Agricultural Machinery*, 5(1): 92-100.

Babai-Ahri, A., R. Golmohammadi, and M. Arzanlou. 2016. Identification of fungal species associated with leaf spot disease on poplar trees (*Populus* spp.) in East Azarbaijan province and some parts of West Azarbaijan and Ardabil provinces. *Applied Researches in Plant Pathology*, 5(2): 105-117.

Bakhshipour-Ziyaratgahi, A., A. A. Jafari, Y. Emam, S. M. Nasiri, S. Kamgar, and D. Zare. 2016. Application of generalized Hough transform for detecting sugar beet plant from weed using machine vision method. *Journal of Agricultural Machinery*, 7(1): 73-85.

Camargo, A., and J. S. Smith. 2009. An image-processing based algorithm to automatically identify plant disease visual symptoms. *Biosystems engineering*, 102(1): 9-21.

Dabbaghi, A., M. H. KhoshTaghaza, M. R. Alizadeh, and H. Zar'eiForoush. 2018. Comparison of common edge detector algorithms to detect edges in non-cracked and rough cracked seeds. Eleventh National Congress on Mechanical Engineering, Biomaterials and Mechanization of Iran. COI: NCAMEM11

Erickson, J. E., G. R. Stanosz, and E. L. Kruger. 2003. Photosynthetic consequences of Marssonina leaf spot differ between two poplar hybrids. *New Phytologist*, 161(2): 577-583.

Fahrentrapp, J., F. Ria, M. Geilhausen, and B. Panassiti. 2019. Detection of gray mold leaf infections prior to visual symptom appearance using a five-band multispectral sensor. *Frontiers in Plant Science*, 10: 628.

Habib, M. T., A. Majumder, A. Z. M. Jakaria, M. Akter, M. S. Uddin, and F. Ahmed. 2020. Machine vision based papaya disease recognition. *Journal of King Saud University-Computer and Information Sciences,* 32(3): 300-309.

Hemming, J., and T. Rath. 2001. PA-Precision agriculture: Computer-vision-based weed identification under field conditions using controlled lighting. *Journal of Agricultural Engineering Research*, 78(3): 233-243.

Izadi, H., S. Kamgar, and M. H. Raoufat. 2016. Tomato grading system using machine vision technology and neuro-fuzzy networks (ANFIS). *Journal of Agricultural Machinery*, 6(1): 49-59.

Lowe, A., N. Harrison, and A. P. French. 2017. Hyperspectral image analysis techniques for the detection and classification of the early onset of plant disease and stress. *Plant Methods*, 13(1): 80.

Maxwell, D. L., E. L. Kruger, and G. R. Stanosz. 1997. Effects of

water stress on colonization of poplar stems and excised leaf disks by *Septoria musiva*. *Phytopathology*, 87(4): 381-388.

Moya, E. A., L. R. Barrales, and G. E. Apablaza. 2005. Assessment of the disease severity of squash powdery mildew through visual analysis, digital image analysis and validation of these methodologies. *Crop Protection*, 24(9): 785-789.

Oberti, R., M. Marchi, P. Tirelli., A. Calcante., M. Iriti., E. Tona, M. Hočevar, J. Baur, J. Pfaff, C. Schütz, and H. Ulbrich. 2016. Selective spraying of grapevines for disease control using a modular agricultural robot. *Biosystems Engineering*, 146: 203-215.

Payman, S. H., A. Bakhshipour-Ziyaratgahi, and A. Jafari. 2016. Exploring the possibility of using digital image processing technique to detect diseases of rice leaf. *Journal of Agricultural Machinery*, 6(1): 69-79.

Polder, G., G. W. van der Heijden, and I. T. Young. 2003. Tomato sorting using independent component analysis on spectral images. *Real-time Imaging*, 9(4): 253-259.

Razavi, M. S., A. Golmohammadi, R. Sedghi, and A. Asghari. 2020. Prediction of bruise volume propagation of pear during the storage using soft computing methods. *Food Science and Nutrition*, 8(2): 884-893.

Rezaei, S., N. Behroozi-Khazaei, and H. Darvishi. 2019. Microwave power adjusting during potato slice drying process using machine vision. *Computers and Electronics in Agriculture*, 160: 40-50.

Yan, T., Z. Hu, Y. Qian, Z. Qiao, and L. Zhang. 2020. 3D shape reconstruction from multifocus image fusion using a multidirectional modified Laplacian operator. *Pattern Recognition*, 98: 107065.

Zhang, S., X. Wu, Z. You, and L. Zhang. 2017. Leaf image based cucumber disease recognition using sparse representation classification. *Computers and Electronics in Agriculture*, 134: 135-141.